CSIT (September 2019) 7(3):191–198
https://doi.org/10.1007/s40012-019-00229-8

S.I. : VISVESVARAYA

Modeling fMRI BOLD signals and temporal mismatches in the cerebellar cortex

Chaitanya Nutakki[1] · Sreedev Radhakrishnan[1] · Bipin Nair[1] · Shyam Diwakar[1]

Received: 27 November 2018 / Accepted: 17 May 2019 / Published online: 24 May 2019

Abstract To understand brain activity relating neurons to circuits to learning and behavior, we explored a bottom-up computational reconstruction of population signals arising from cerebellum granular layer. As a first implementation, using bio-realistic computational models of cerebellum granule cell, in vivo spike train patterns were computed and then translated into functional Magnetic Resonance Imaging, Blood Oxygen-Level Dependent (BOLD) signals. The BOLD response was generated from averaged activity arising from center-surround organization modeled by using excitatory-inhibitory ratios related to experimental data. The averaged responses were converted to BOLD signals using the balloon and modified Windkessel models. Although both models generated BOLD responses corresponding to neural activity, the temporal mismatch was attributed to the response by the delayed compliance parameter in the Windkessel model. The modeling suggests that experimental variability observed in the cerebellar micro-zones could be related to compliance chances, activation patterns and number of neurons. Although detailed neuro-vasculature information was not modeled, the advantage in this methodology is that cerebellar cortex may allow seemingly linear transformations of underlying spiking that could be then used to validate network reconstructions.

Keywords Computational neuroscience · fMRI · BOLD · Mathematical modelling · Neural activity

✉ Shyam Diwakar
shyam@amrita.edu

[1] Amrita School of Biotechnology, Amrita Vishwa Vidyapeetham, Amritapuri Campus, Kollam, Kerala, India

1 Introduction

With complexity from nonlinear responses attributed to neural activity and their emergent behaviors, computational modeling in neuroscience relates translational and clinically-relevant interpretations through bottom-up and top-down approaches. With experimental data, mathematical reconstructions also impact testing treatment paradigms for neurodegenerative disorders. Among human brain activity imaging techniques, the functional magnetic resonance imaging (fMRI), is often used to understand circuit function through correlations of hemodynamic changes for inter-connecting tasks or resting-states related brain function and dysfunction. Changes in CBV (cerebral Blood volume) CMRO2 (cerebral metabolic rate oxygen) cerebral blood flow (CBF) and dhb (deoxyhemoglobin) in the activated region of the brain [1, 2] coupled with metabolic changes are seen through fMRI Blood Oxygen-Level Dependent (BOLD) signals with respect to neural activity [3].

To reconnect cellular activity to neuronal population activity and further to BOLD responses relating to observations in clinical settings [4], cellular activity to ensemble response need to be modeled from a bottom-up approach. Predictions arising from neural activity allow analyzing phases of BOLD signal including onset of the stimulus [5], overshoot, and post stimulus undershoot with respect to the neural activity [6]. Experimentally, BOLD responses not only depends on the oxygenated blood but also the CBV (cerebral blood volume), CBF Cerebral blood flow changes [7–9].

Cerebellum, a brain structure in all vertebrates, is critically attributed to how timing and motor strategies are implemented in the brain and related to motor coordination [10], timing [11–13], movement execution [14, 15] among

other roles and functions. Failures in cerebellar circuits are attributed to several cognitive and movement-related disorders and conditions [16] including spino-cerebellar ataxia [17], Alzheimer's dementia [18], Parkinson's disease [19] and autism [20]. Previous studies had developed detailed and spiking models of cerebellum cells [21, 22] and circuits relating input signals entering the cerebellum granular layer. Neuronal pathways and circuits that controls the blood supply in the cerebellum are unclear. Also, granule cells are numerous and most energy consuming neurons in the cerebellum [23]. The activated granular neurons with metabolic demand causes vasodilation through neuronal nitric oxide synthase (nNOS) and NMDA receptors expression helps in effective cerebellar neuro vascular coupling [24–26]. Capillary diameter changes in mossy fiber stimulated acute rat cerebellar slices have been demonstrated in [27].

Towards the goal of connecting modeled neural behavior to dynamics at the behavioral level as seen in fMRI, a dynamic model that predicts the volume changes in the venous compartment was modelled. Temporal mismatches happen due to changes in blood flow-neural activity relations. Rate change of volume was modelled as a difference in inflow and outflow of the compartment with respect to time [1]. Flow volume relationship was modelled as a capacitance and resistance [28]. However, a modification by incorporating delayed compliance was able to capture the dynamic changes of CBF and CBV in increase and while returning to the baseline [29]. As alternatives to bottom-up methods, dynamic causal modeling, another biomechanical modeling approach helps to understand the brain function from the hidden neural states [30, 31].The dynamic causal model was introduced for fMRI data analysis helps to model the neuronal population responses [31, 32]. In literature, to reduce complexity, two-state DCM approach have also been used to model hemodynamic response changes among neuronal regions [33]. However, unlike detailed reconstructions in bottom-up methods, top-down causal models need several assumptions.

Extracting spatio-temporal activity in the cerebellum granular circuitry help reveals the functional features of the input layer network with respect to time [34, 35]. Towards that goal, this paper focusses on relating a bottom-up approach in computational neuroscience, i.e., by reconstructing large-scale fMRI BOLD signals from detailed biophysical neurons and experimentally validated circuit topographies in order to relate cellular activity to ensemble responses.

2 Methods

2.1 Modeling neuronal response from granular layer network

Detailed multicompartmental granule cell model [21] consisting 52 active compartments, namely, a soma, 4 dendrites with 4 compartments, 5 hillock compartments and 30 compartment axon based on electrophysiological data from p19-23 Wistar rats was employed. The model was simulated for 1000 ms.

In this study, a common spatio-temporal organization of the cerebellum granular layer, namely the center-surround pattern showing that excitation and inhibition spreading from the center to the periphery [36] was reconstructed. The excitatory inputs from the mossy fibers and inhibitory stimuli from Golgi cells were modeled to reconstruct in vitro (acute brain slices) and in vivo (anaesthetized) activity [21]. As in in vivo experiments [37], it was considered that (15%) of the neurons from the center shared 4 inhibitory and excitatory mossy fiber inputs, 35% of cells receives 3 inhibitory and excitatory mossy fiber synapse, 15% receives 2 mossy fiber inhibitory and excitatory inputs and 35% of cells receives 1 inhibitory and excitatory mossy fiber inputs simulated different firing frequencies and inter-spike intervals at invivo condition for 1000 ms. For each of the inhibitory synapses, inter-spike interval and inter-burst interval was maintained at 10 ms and 300 ms with delay of 24 ms (attributing the time-window in mossy fiber- Golgi cell-granule cell loop, see [38]). Whereas for excitatory synapse inter-spike interval and inter-burst interval was set at 2 ms and 300 ms with delay of 20 ms.

2.2 Estimating averaged responses from neural spike trains

Spike trains were extracted for each model neuron (see Fig. 1a) in order to generate the averaged spike responses that were used to relate to BOLD response (Fig. 1b). Average spike trains were calculated by mapping each spike train to a specific kernel function and then averaging each function to get the best corresponding spike train. Given a spike train

$$\mathbf{s} = \{s_1, s_2, \ldots, s_m\} \tag{1}$$

Spike trains are then mapped into a real function f(t; s) Eq. 2, using a kernel k (t). Where t is the time with respect to spike s. Kernel function is defined as Eq. 3

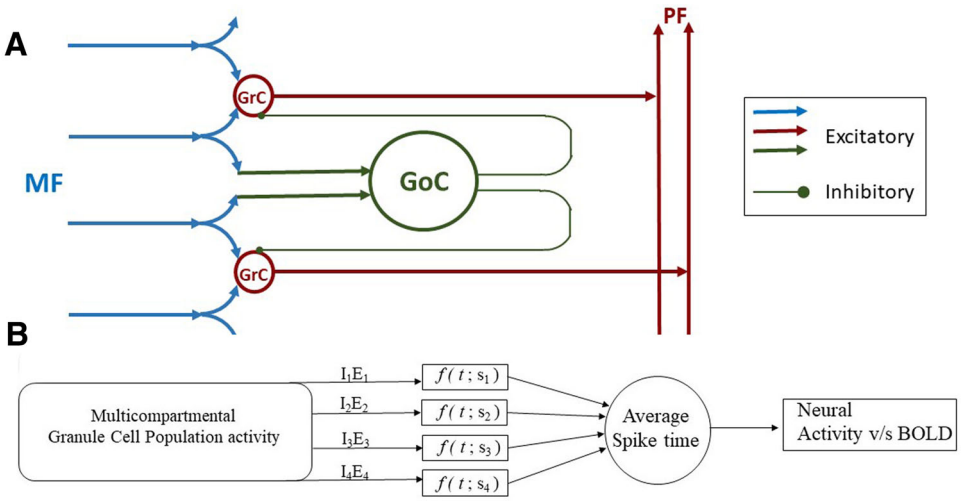

Fig. 1 Schematic representation of cerebellar granular layer BOLD extraction. **a** Representation of cerebellar granular layer (GrC- Granule cell, GoC-Golgic cell, and MF-Mossy fiber, PF-Parallel fibers. **b** BOLD estimation from average spike trains

$$\mathbf{s} \mapsto f(t;\mathbf{s}) = \sum_{i=1}^{m} k(t - \mathbf{s}_i) \tag{2}$$

Kernel function is specified as

$$k(t) = \begin{cases} 0, & t < 0 \\ \left(\sqrt{\frac{2}{\tau}} e^{-t/\tau}\right) & t \geq 0 \end{cases} \tag{3}$$

A collection of spike trains are taken and are averaged to Eq. 4. Where $\bar{f}(t)$ represents the average of all the spike trains, 'n' represents the number of spike trains.

$$\{f(t;\mathrm{s}_1), (t;\mathrm{s}_2), \ldots, f(t;\mathrm{s}_n)\} \tag{4}$$

$$\bar{f}(t) = \frac{1}{n}\sum_{I=1}^{n} f(t;\mathbf{s}_I) \tag{5}$$

2.3 Reconstructing BOLD response in cerebellar granular layer

BOLD responses were calculated using Balloon and modified Windkessel models [28, 39]. Hemodynamic model was developed that correlates the neural activity and corresponding BOLD response. The current model was a combination of balloon and Windkessel model and included a set of ordinary differential equations that governed the BOLD response, y(t), in terms of, blood flow (fin) total cerebral blood volume (V), total deoxyhemoglobin (q) and v(f) recovery of Vi after stimulus. The change in the volume was modelled as the difference between the flow in and flow out of the compartment. In the modified Windkessel model by adapting the delayed compliance helps to model pressure flow mechanism into the compliant vessels [4].

3 Results

3.1 Electroresponsiveness properties attribute to population activity in the granular layer

The multicompartmental granule cell model was simulated for 1000 ms using the centre-surround activation pattern (See Fig. 2). Among 220 cells, 33 cells near centre received the strong excitatory (E) and inhibitory (I) stimuli (I4E4), and consecutive peripheral neurons receives I3E3 for 77 cells, 33 cells receive I2E2 and 77 cells receive I1E1. Firing behaviour of the network was simulated providing in vivo like condition. The extracted granule cell neural activity was taken and corresponding BOLD activity was generated using modified Windkessel model with different frequencies and bursts (Fig. 2) with same temporal scale.

Presence of the delayed compliance in modified Windkessel model showed a significance in volume and BOLD responses, particularly during the return to the base line. The strength of the BOLD signal was based on the stimulation time. The initial dip and raise of BOLD signal according to the stimulus and the post stimulus undershoot was modelled through the compliance variable (Fig. 2b, d, f, h). Not all of individual neural activity was seen in the single neuron—BOLD reconstruction.

3.2 Reconstructed BOLD response from averaged bio-realistic spike trains

The spike trains were mapped to a function using a kernel, and summed up activity of all the spike trains were taken as an averaged response (Fig. 3). BOLD response was modelled using modified Windkessel model correlates the averaged population activity of the granule cells (Fig. 3b). Transient features of BOLD response was proportional to

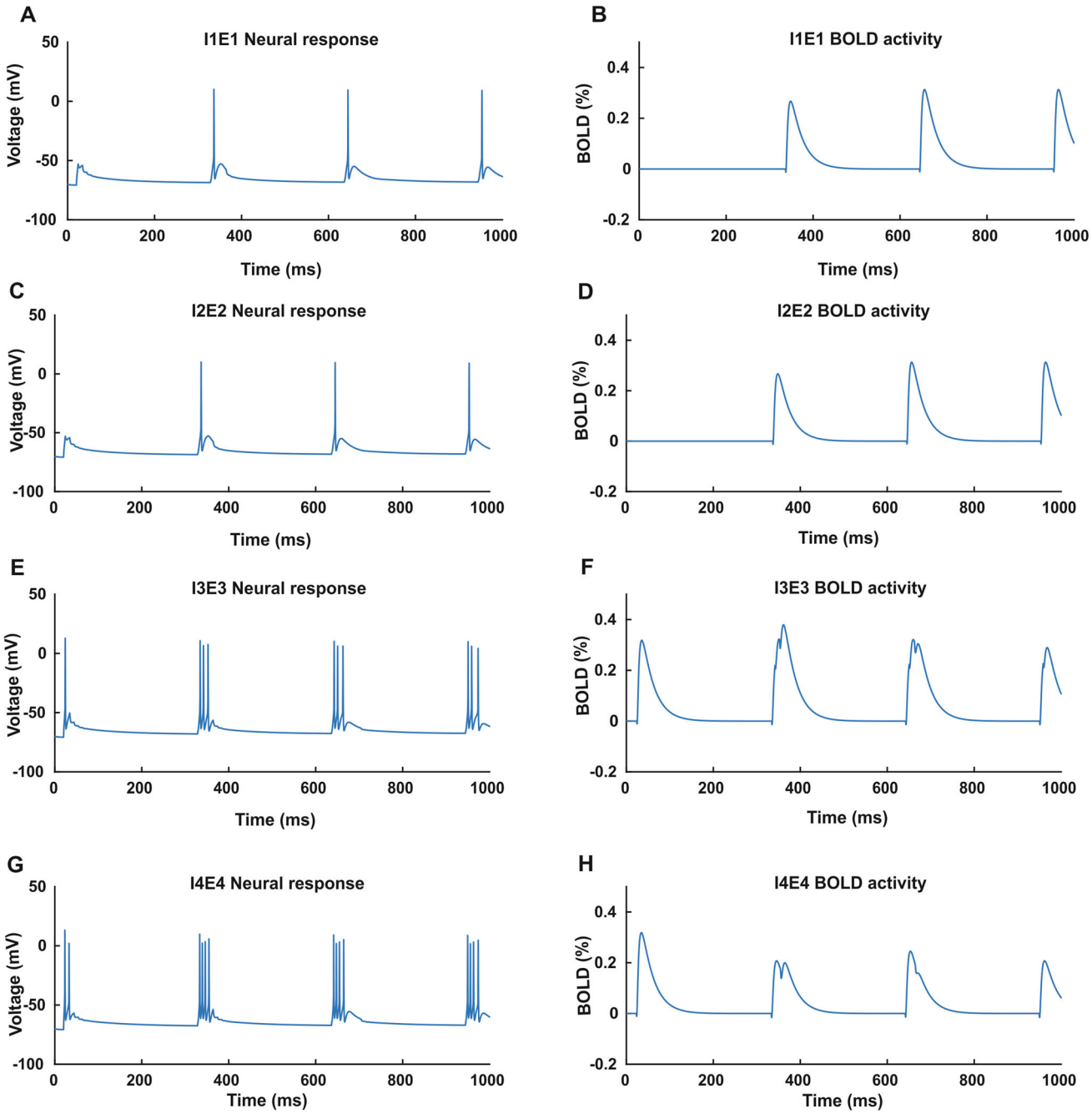

Fig. 2 Reconstructing Cerebellar granular layer neural activity and the corresponding BOLD response. **a** Multicompartmental granule cell activity by providing 1 inhibitory and 1 excitatory (I1E1) synapse. **b** BOLD response for (I1E1) spike activity. **c** Multicompartmental granule cell activity by providing 2 inhibitory and 2 excitatory (I2E2) synapses. **d** BOLD response for (I2E2) spike activity. **e** Multicompartmental granule cell activity by providing 3 inhibitory and 3 excitatory (I3E3) synapse. **f** BOLD response for (I3E3) spike activity. **g** Multicompartmental granule cell activity for 4 inhibitory and 4 excitatory (I4E4) synapses. **h** BOLD response for (I4E4) spiking activity

the temporal changes in the flow and volume. The averaged response also allowed to attribute similarities in blood flow-related changes rather than single neuron responses attributing a seemingly linear behavior of response at the population scale. The averaging could also suggest a correlation to changes observed in neuro-vascular coupling as observed in [27]. Through modeling, neural activity (NA)-induced NO was reconstructed by the synaptic excitation patterns to the granule cell (data not shown). At steady-state and nonactivated state, NO concentration remained same, when neuronal nitric oxide synthase was activated by increased neural activity changes to NO followed the

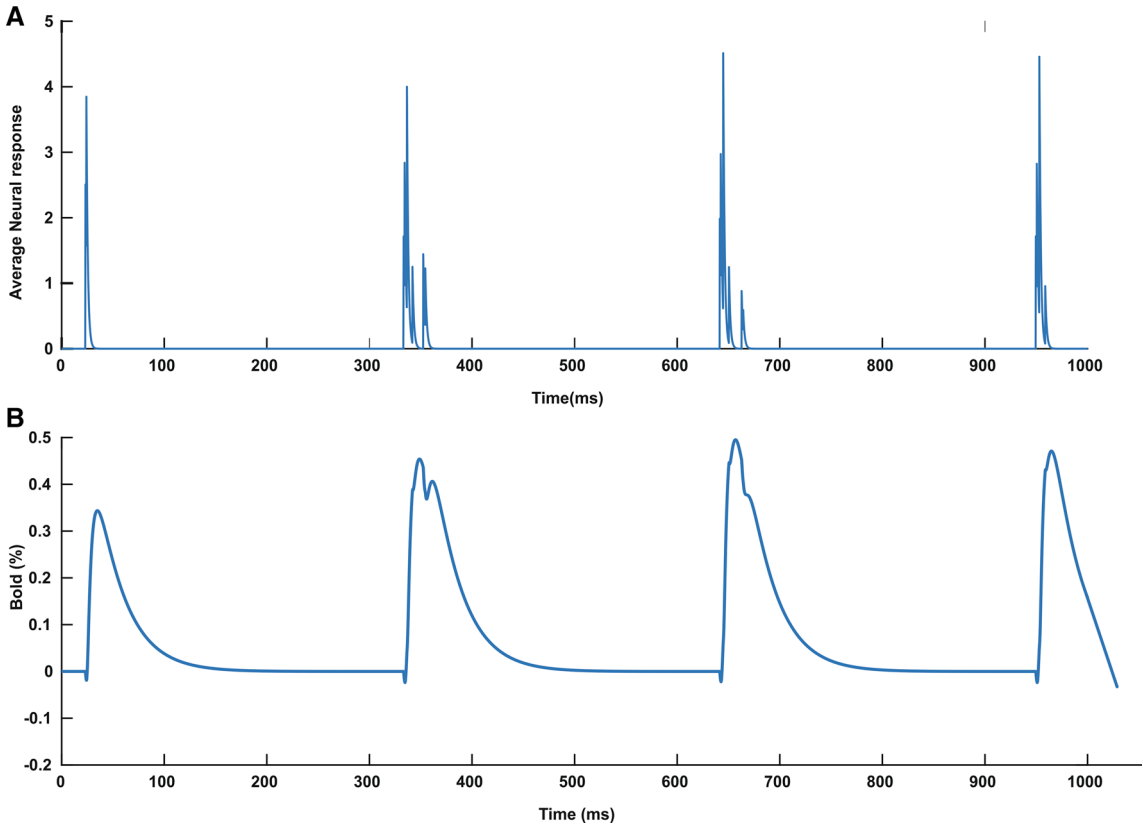

Fig. 3 Averaged neural activity and corresponding BOLD response. The reconstruction shows the depolarization of the BOLD response to the neural timing whereas the shape of the response was shaped by multiple parameters including number of spikes, compliance and time delays. Averaged activity attributes similarities to nitric oxide changes in the cerebellar granular layer [27]

duration of the stimuli with a delayed compliance for initial activation.

3.3 Computational reconstructions of fMRI BOLD and flow-related temporal mismatch from neural activity

Translating neural activity to blood inflow (fin) was performed using a trapezoidal function and convolved with the hemodynamic response function to generate the BOLD signal with a simulation time of 1 s using modified Windkessel and balloon models. BOLD, CBV changes were reconstructed during the onset of stimulation and after the stimuli with respect to the baseline and peak values (Fig. 4). Same stimuli was used for both balloon (Fig. 4a, b) and Windkessel models to generate the temporal mismatch of flow and volume as delayed compliance in the model (Fig. 4c, d). The specific relation to various lobes of cerebellum may involve variations through delayed compliance as indicated through the comparison between balloon (Fig. 4b) and modified Windkessel (Fig. 4d) reconstructions.

4 Discussion

As part of this study, we explored reconstructing fMRI BOLD responses in the cerebellar granular layer using the balloon and modified Windkessel models. For densely populated neural regions such as circuits in the cerebellum, there may be a seemingly linear relationship between overall activity and nature of generated BOLD response. The subset of activation patterns within the context of center-surround excitation geometries were relevant since underlying granule neurons could elicit a simultaneous shaping of Purkinje neuron's response and this could attribute to variations in BOLD across multiple regions in the cerebellum granular layer.

A comparison was performed on the balloon and modified Windkessel models for cerebellum granular layer inputs suggests blood volume and BOLD returns to the baseline much slower than the blood flow. The modified Windkessel model implementation suggests the temporal mismatch variability in cerebellar microzones as suggested in some studies could be also attributed to the delayed compliance that may need to include circumference stress relaxation models for blood vessels in the cerebellar cortex. BOLD post stimulus undershoot phenomena seems related

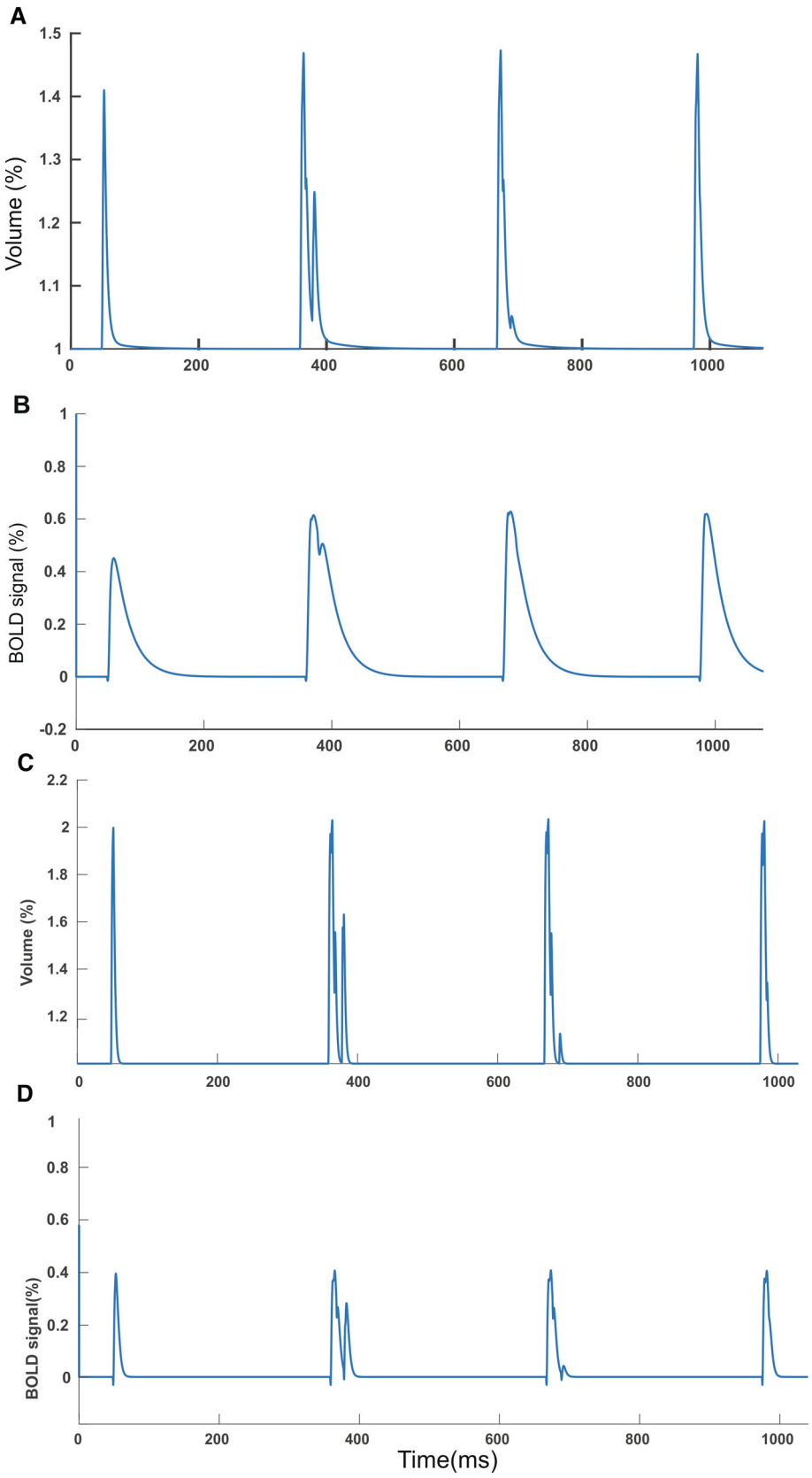

Fig. 4 Comparison of reconstructed BOLD and blood flow volumes using balloon and modified Windkessel model. While **a** and **c** represent changes in blood volumes with neural activity, the balloon model reconstruction (**b**) and Modified Windkessel model reconstruction involving delayed compliance (**d**) show significant time delays in reaching baseline

to the delayed compliance and could be substituted with simpler state variables for large-scale modeling.

With delayed compliance, the BOLD response in the cerebellar cortex returned to the baseline much faster than the data which was not significant using the balloon model. It may be relevant for the densely-packed circuits such as the cerebellar cortex in order to related neural activity to emergent responses, a combined balloon and modified Windkessel model need to be used with averaging taking into consideration the jitter delays and excitation similarity in neuronal subpopulations.

Towards bottom-up modelling, reconstructing temporal structure will need more detailed experimental validations of the neurovascular components that surface in BOLD responses. With close approximations, it may be then possible to reconnect top-down (dynamic causal) models and bottom-up modelling approaches allowing a better insight into translational neurosciences and specifically, relating circuit functions and dysfunctions to underlying cells and their activity.

5 Conclusion

As an ongoing study, using detailed mathematical models, a bottom-up modelling, of cerebellar BOLD responses suggests neural activity in cerebellar cortex can be scaled and approximated while connecting multiple scales within such circuits. This style of modelling has more than physiological roles. It may help abstract large-scale brain activity to validate network models, design experimental interventions such as sodium channel modulations during plasticity, effect of pharmacological drugs and as readouts for robotic abstractions controlled by cerebellum-inspired pattern recognition models.

Acknowledgements This work derives direction and ideas from the Chancellor of Amrita Vishwa Vidyapeetham, Sri Mata Amritanandamayi Devi. This work was supported by Visvesvaraya Young Faculty Research Fellowship from Digital India Corporation, Ministry of Electronics and IT, Government of India and partially by grant DST/CSRI/2017/31 from the Department of Science and Technology, Government of India and by Embracing The World.

References

1. Buxton RB, Wong EC, Frank LR (1998) Dynamics of blood flow and oxygenation changes during brain activation: the balloon model. Magn Reson Med 39(6):855–864
2. Ekstrom A (2010) How and when the fMRI BOLD signal relates to underlying neural activity: the danger in dissociation. Brain Res Rev 62(2):233–244
3. Shen Q, Ren H, Duong TQ (2008) CBF, BOLD, CBV, and CMRO2 fMRI signal temporal dynamics at 500-msec resolution. J Magn Reson Imaging 27(3):599–606
4. Nutakki C, Nair A, Medini C, Nair M, Nair B, Diwakar S (2016) Computational reconstruction of fMRI-BOLD from neural activity. In: 2016 International conference on advances in computing, communications and informatics (ICACCI), pp. 922–926
5. Kwong KK et al (1992) Dynamic magnetic resonance imaging of human brain activity during primary sensory stimulation. Proc Natl Acad Sci 89(12):5675–5679
6. Buxton RB (2001) The elusive initial dip. Neuroimage 13(6):953–958
7. Boxerman JL et al (1995) The intravascular contribution to fMRI signal change: Monte Carlo modeling and diffusion-weighted studies in vivo. Magn Reson Med 34(1):4–10
8. Buxton RB, Frank LR (1997) A model for the coupling between cerebral blood flow and oxygen metabolism during neural stimulation. J Cereb Blood Flow Metab 17(1):64–72
9. Ogawa S, Menon RS, Kim S-G, Ugurbil K (1998) On the characteristics of functional magnetic resonance imaging of the brain. Annu Rev Biophys Biomol Struct 27(1):447–474
10. Koziol LF et al (2014) Consensus paper: the cerebellum's role in movement and cognition. Cerebellum 13(1):151–177
11. D'Angelo E, De Zeeuw CI (2008) Timing and plasticity in the cerebellum: focus on the granular layer. Trends Neurosci 32(1):30–40
12. Mauk MD, Medina JF, Nores WL, Ohyama T (2000) Cerebellar function: coordination, learning or timing? Curr Biol 14:522–525
13. Ivry RB, Spencer RM, Zelaznik HN, Diedrichsen J (2002) The cerebellum and event timing. Ann N Y Acad Sci 978:302–317
14. Chen S, Augustine GJ, Chadderton P (2016) The cerebellum linearly encodes whisker position during voluntary movement. Elife 5(JANUARY2016):1–16
15. Proville RD et al (2014) Cerebellum involvement in cortical sensorimotor circuits for the control of voluntary movements. Nat Neurosci 17(9):1233–1239
16. Rajendran A, Nutakki C, Sasidharakurup H, Bodda S, Nair B, Diwakar S (2017) Cerebellum in neurological disorders: a review on the role of inter-connected neural circuits. J Neurol Stroke 6(2):1–4
17. Rinaldo L, Hansel C (2010) Ataxias and cerebellar dysfunction: involvement of synaptic plasticity deficits? Funct Neurol 25(3):135–139
18. Castellazzi G et al (2014) A comprehensive assessment of resting state networks: bidirectional modification of functional integrity in cerebro-cerebellar networks in dementia. Front Neurosci 8:223
19. Yu H, Sternad D, Corcos DM, Vaillancourt DE (2007) Role of hyperactive cerebellum and motor cortex in Parkinson's disease. Neuroimage 35(1):222–233
20. Schmahmann JD (1998) Dysmetria of thought: clinical consequences of cerebellar dysfunction on cognition and affect. Trends Cogn Sci 2(9):362–371
21. Diwakar S, Magistretti J, Goldfarb M, Naldi G, D'Angelo E (2009) Axonal Na + channels ensure fast spike activation and back-propagation in cerebellar granule cells. J Neurophysiol 101(2):519–532
22. Medini C, Vijayan A, D'Angelo E, Nair B, Diwakar S (2014) Computationally efficient bio-realistic reconstructions of cerebellar neuron spiking patterns. In: International conference on interdisciplinary advances in applied computing, Amrita University, Coimbatore, India
23. Howarth C, Peppiatt-Wildman CM, Attwell D (2010) The energy use associated with neural computation in the cerebellum. J Cereb Blood Flow Metab 30(2):403–414
24. Snyder SH (1992) Nitric oxide: first in a new class of neurotransmitters. Science 257(5069):494–496
25. Garthwaite J, Garthwaite G (1987) Cellular origins of cyclic GMP responses to excitatory amino acid receptor agonists in rat cerebellum in vitro. J Neurochem 48(1):29–39

26. Garthwaite J, Garthwaite G, Palmer RMJ, Moncada S (1989) NMDA receptor activation induces nitric oxide synthesis from arginine in rat brain slices. Eur J Pharmacol Mol Pharmacol 172(4–5):413–416
27. Mapelli L, Gagliano G, Soda T, Laforenza U, Moccia F, D'Angelo EU (2017) Granular layer neurons control cerebellar neurovascular coupling through an NMDA receptor/NO-dependent system. J Neurosci 37(5):1340–1351
28. K. J. Friston, A. Mechelli, R. Turner, and C. J. Price (2000) Nonlinear responses in fMRI: the Balloon model, Volterra kernels, and other hemodynamics. NeuroImage, [Online]. http://www.ncbi.nlm.nih.gov/pubmed/10988040. Accessed 07 Mar 2013
29. Kong Y et al (2004) A model of the dynamic relationship between blood flow and volume changes during brain activation. J Cereb Blood Flow Metab 24(12):1382–1392
30. Stephan KE, Penny WD, Moran RJ, den Ouden HEM, Daunizeau J, Friston KJ (2010) Ten simple rules for dynamic causal modeling. Neuroimage 49(4):3099–3109
31. Friston KJ, Harrison L, Penny W (2003) Dynamic causal modelling. Neuroimage 19(4):1273–1302
32. Friston K (2009) Causal modelling and brain connectivity in functional magnetic resonance imaging. PLoS Biol 7(2):e1000033
33. Marreiros AC, Kiebel SJ, Friston KJ (2008) Dynamic causal modelling for fMRI: a two-state model. Neuroimage 39(1):269–278
34. D'Angelo E, De Zeeuw CI (2009) Timing and plasticity in the cerebellum: focus on the granular layer. Trends Neurosci 32:30–40
35. Solinas S, Nieus T, D'Angelo E (2010) A realistic large-scale model of the cerebellum granular layer predicts circuit spatio-temporal filtering properties. Front Cell Neurosci 4:12
36. Medini C, Nair B, D'Angelo E, Naldi G, Diwakar S (2012) Modeling spike-train processing in the cerebellum granular layer and changes in plasticity reveal single neuron effects in neural ensembles. Comput Intell Neurosci 2012:359529
37. Diwakar S, Lombardo P, Solinas S, Naldi G, D'Angelo E (2011) Local field potential modeling predicts dense activation in cerebellar granule cells clusters under LTP and LTD control. PLoS One 6(7):e21928
38. D'angelo E et al (2011) The cerebellar network: from structure to function and dynamics. Brain Res 66(1–2):1–11
39. Medini C, Vijayan A, D'Angelo E, Nair B, Diwakar S (2014) Computationally efficient biorealistic reconstructions of cerebellar neuron spiking patterns. In: International Conference on Interdisciplinary Advances in Applied Computing—ICONIAAC'14, pp. 1–6